GFZ

Helmholtz Centre POTSDAM

Detailed seismicity analysis revealing the dynamics of the southern Dead Sea area

DESIRE

Braeuer B.*, Asch G., Haberland C., Weber, M. (GeoForschungsZentrum (GFZ), Germany), Hofstetter R. (Geophysical Institute of Israel (GII)), Darwish J. (Natural Resources Authority (NRA), Jordan)

El-Kelani R. (An-Najah National University, Palestine) and DESIRE GROUP; *ben@gfz-potsdam.de

Abstract

While the Dead Sea basin has been studied for a long time, the available knowledge about the micro-seismicity, its distribution and characteristics is limited. Therefore, within the framework of the international DESIRE (DEad Sea Integrated REsearch) project, a dense temporary local seismological network was operated in the southern Dead Sea area. Within 18 month of recording 650 events were detected. Based on an already published tomography study clustering, focal mechanisms, statistics and the distribution of the micro-seismicity in relation to the velocity models from the tomography are analyzed. The determined b-value of 0.7 indicates a relatively high risk of large earthquakes compared to the moderate microseismic activity. The distribution of the seismicity indicates an asymmetric basin with a vertical strike slip fault forming the eastern boundary of the basin, and an inclined western boundary, made up of strike-slip and normal faults. Furthermore, significant differences between the area North and South of the Bokek fault were observed. South of the Bokek fault the western boundary is inactive while the entire seismicity occurs at the eastern boundary and below the basin-fill sediments. The largest events occurred here, their focal mechanisms represent the northwards transform motion of the Arabian plate along the Dead Sea Transform. The vertical extension of the spatial and temporal cluster from February 2007 is interpreted as being related to the locking of the region around the Bokek fault. North of the Bokek fault similar seismic activity occurs at both boundaries most notably within the basin-fill sediments, displaying mainly small events with strike-slip mechanism and normal faulting in EW direction. Therefore, we suggest that the Bokek fault forms the border between the "single" transform fault and the pull-apart basin with two active border faults.

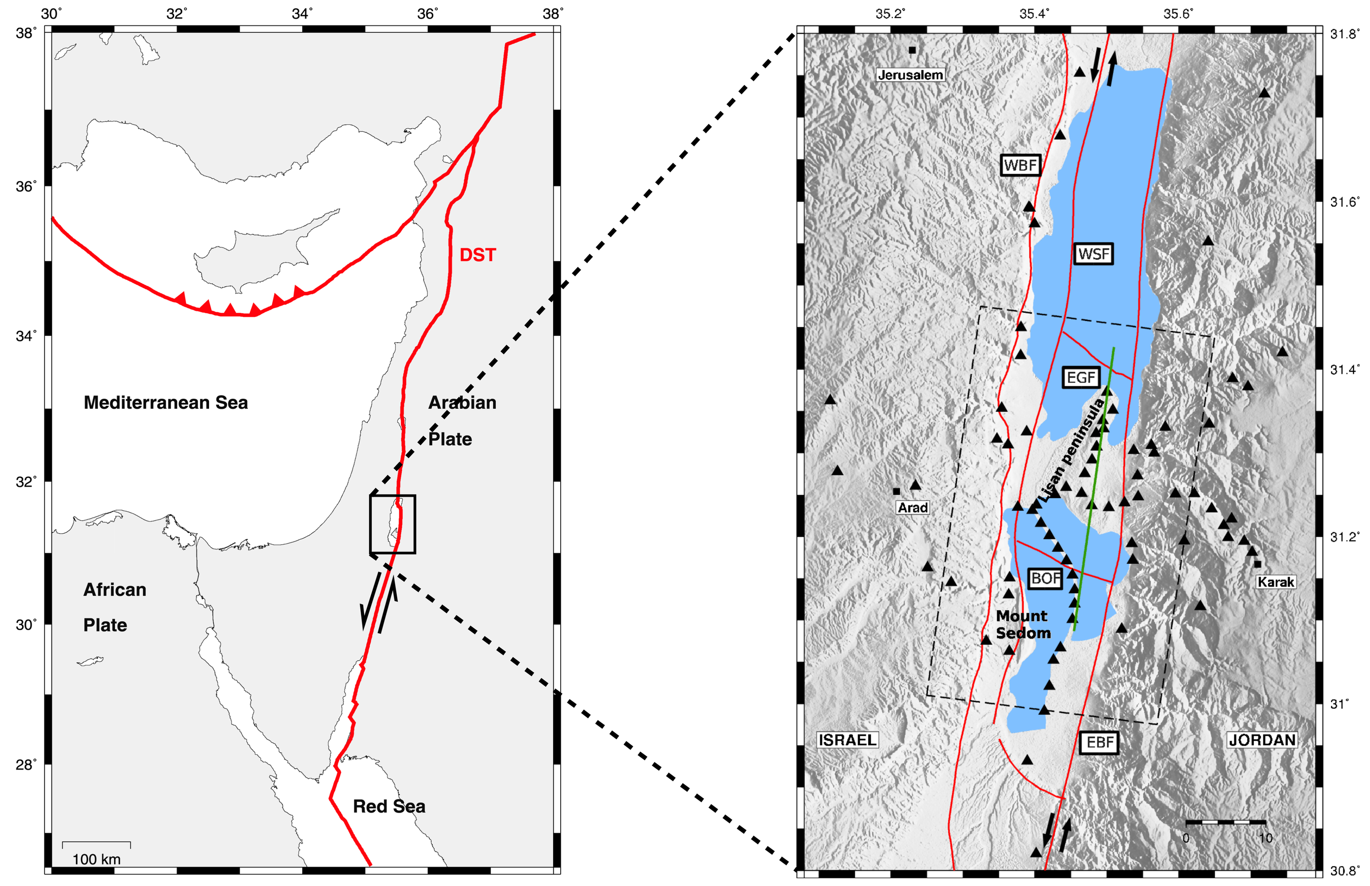

Fig. 1 Left: Overview of the plate boundaries in the region around the Dead Sea. The left lateral moving (107 km within the last 20Ma) Dead Sea Transform (DST) separates the Arabian plate from the African plate. Right: 65 seismic stations were recording the microseismicity in the southern Dead Sea area between October 2006 and March 2008. Only the main faults are indicated as solid red lines. Eastern border fault (EBF); Western strike-slip fault (WSF) and Western Boundary fault (WBF), here collectively called Western faults (WF). The two faults bordering the Lisan diapir: Ein Gedi fault (EGF), Bokek fault (BOF). The green line is indicating the North-South - profile of Figure 10. The dashed box is indicating the study area in (Figure 11a).

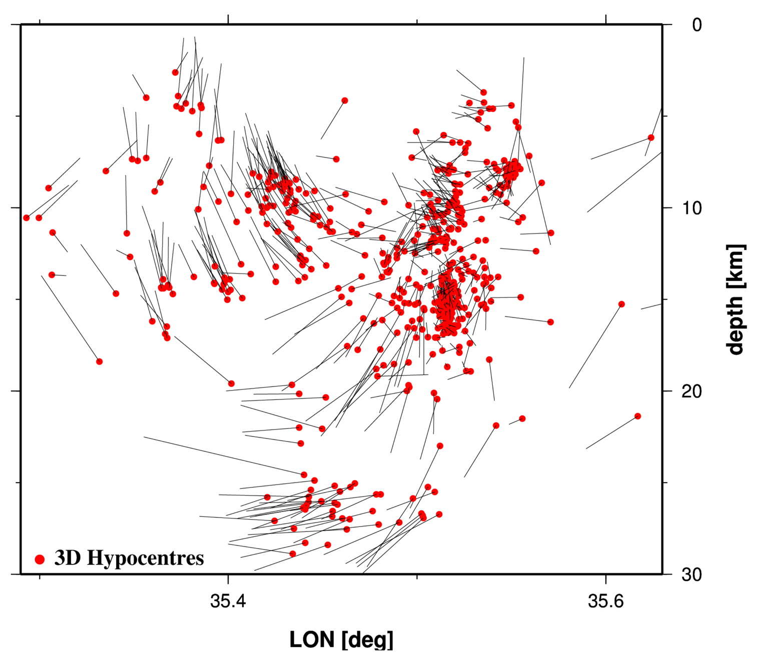

Fig. 2 Longitude - depth section with vectors indicating the shift in hypocentre location after the tomographic v_P and v_P/v_S inversions (indicated by red circles) relative to hypocentre location obtained with the 1D model. The difference between the velocities in the 1-D model and the tomographic models of up to +/- 25 % (Braeuer et al. 2012) results in large location discrepancy of 3-5 km. Therefore, a new inspection of the distribution of the seismicity was done.

Fig. 3 Upper crustal seismic activity at the western (left) and eastern (right) boundaries displayed in depth vs. latitude. The red-dashed boxes in both diagrams are indicating the seismic active area at the eastern boundary; South of 31.15°N (A, South of the BOF), between between 31.15°N and 31.4°N (B, between BOF and EGF) and North of 31.4°N (EGF). In the south only the eastern boundary is active (A). Meanwhile between 31.15°N and 31.4°N the behaviour of both boundaries looks similar (B). At 31.2°N seismicity occurs between 4 and 12 km depth. Northwards the lower boundary is increasing continuously to 17 km depth at around 31.4°N f or both faults. North of 31.4°N, towards the end of the study area, the seismicity at the EBF is concentrated around 8 km depth, while at the western faults events occur between 13 and 20 km depth. Thus, the behaviour seems to again be different at each boundary (eastern and western boundary) north of 31.4°N.

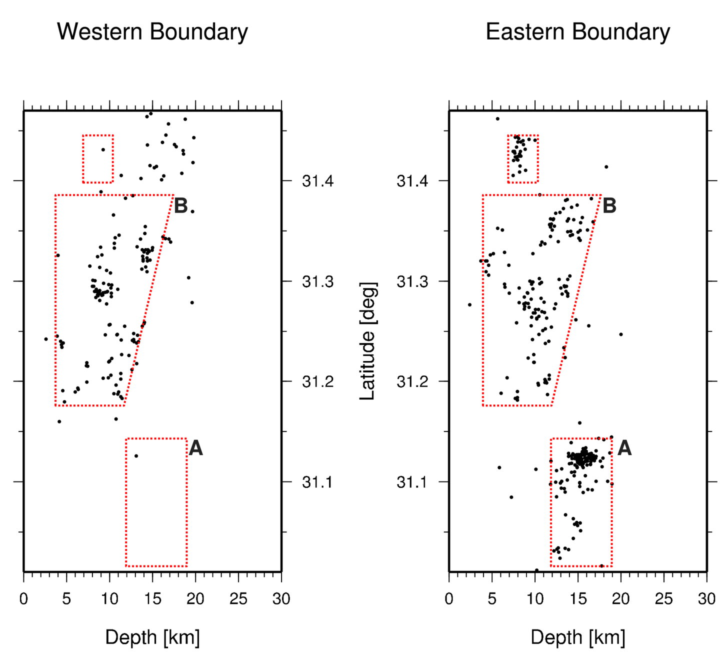

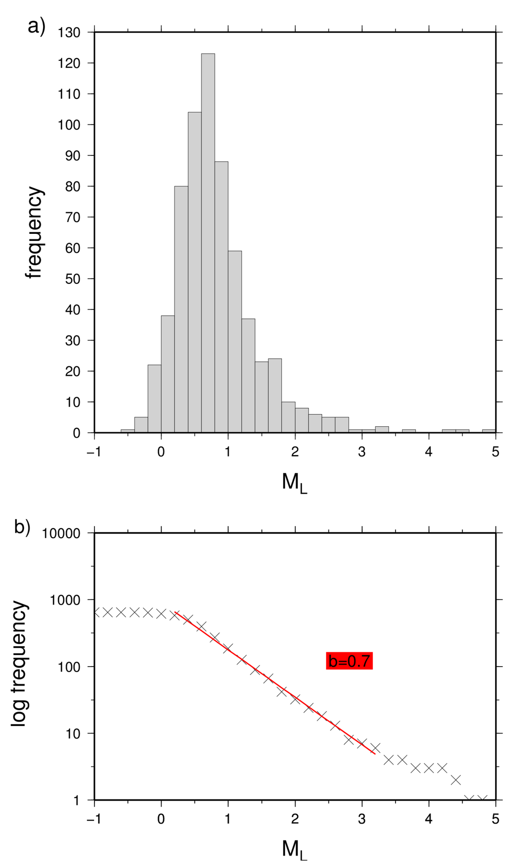

Fig. 4 Linear (a) and cumulative-logarithmic (b) representation of the frequency of events per 0.2 Magnitude M_L.
In addition to the 530 events used for the tomographic inversion (Braeuer et al., 2012), we determined local magnitudes M_L for 116 events. This dataset of 646 events was used to determine the b-value by a simple line-fit of the linear part of the logarithmic magnitude-frequency distribution (Figure [fig: b-value]). For events in the range of $-0.5 < M_L < 4.8$ a completeness magnitude of $M_C = 0.4$ was revealed. The resulting b-value of 0.7 is smaller than older values of 0.8 (for the DSB, Shapira and Feldman, 1987) and 0.97 (for the entire DST, Hamiel et al., 2009).

Fig. 5 Location of fault plane solutions indicated as red dots in a depth - latitude section. A: Events south of 31.15°N. B: Events in the upper crust north of 31.15°N. C: Events in the lower crust north of 31.15°N. 11 of 30 events, where focal plane determination was possible, occurred in the Southeast of the study area (A, see also Figure 3). The largest events occurred there and almost all events are showing strike-slip mechanism with fault planes oriented West-East and North-South, reflecting the regional stress regime. The events in the upper crust in the north (B, occurred at both boundaries, see Figure 3) show strike-slip mechanisms, West-East oriented normal faulting character, or a mixture of both. The highest magnitudes archived by events in the north is one magnitude smaller than the largest events in the South. The few events in the lower crust show strike-slip mechanisms and normal faulting (C).

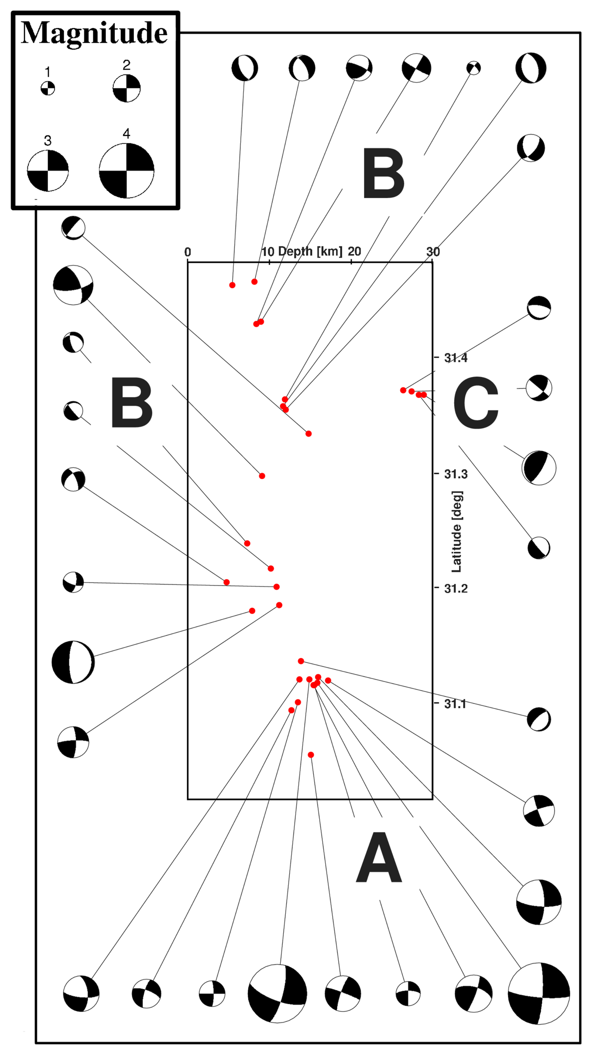

Cluster

Between February, 9th 2007 and March, 4th 2007, 115 events occurred in a very small area in the southeast of the basin in the depth range of 14 and 17 km (red square Figure 11a). While the entire earthquake sequence related to that cluster lasted 24 days, half of the events occurred within the first 7 hours (Figure 6).The first and the third events were among the largest of all events during the recording period (ML of 4.3 and 4.5, respectively). 4 other events display magnitudes larger than 2.5, and all the other events had magnitudes between 0.5 and 2 (Figure 7). The events of the cluster were relocated using the double-difference location procedure HypoDD (Waldhauser et al. 2001). The accuracy of the locations is significantly improved by including time differences determined by cross correlation. Fig. 8 shows that the events have similar epicenters, only the depth (14.5-17km) differs between them. The cluster shows hence a vertical structure perpendicular to the direction of the movement on the main faults (horizontally North-South). A potential dependency between origin time and depth, indicating fluid induced seismicity was tested, but could not be confirmed. An approach to verify that the cluster has a first order vertical structure is presented in Figure 9.

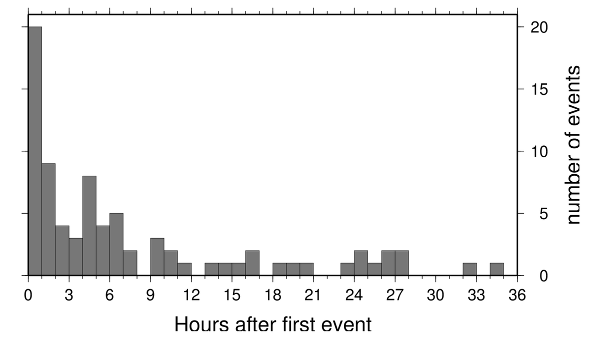

Fig. 6 Number of events per hour after the first event of the cluster.

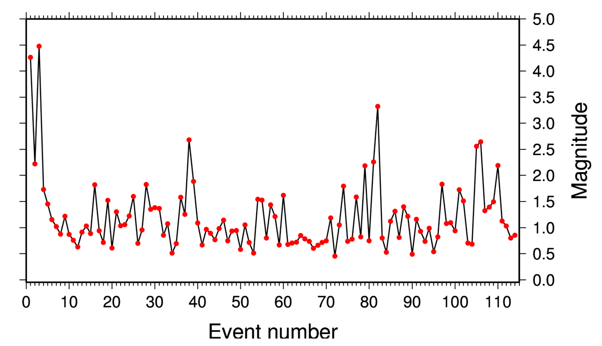

Fig. 7 Magnitude of the events in the cluster in chronological order.

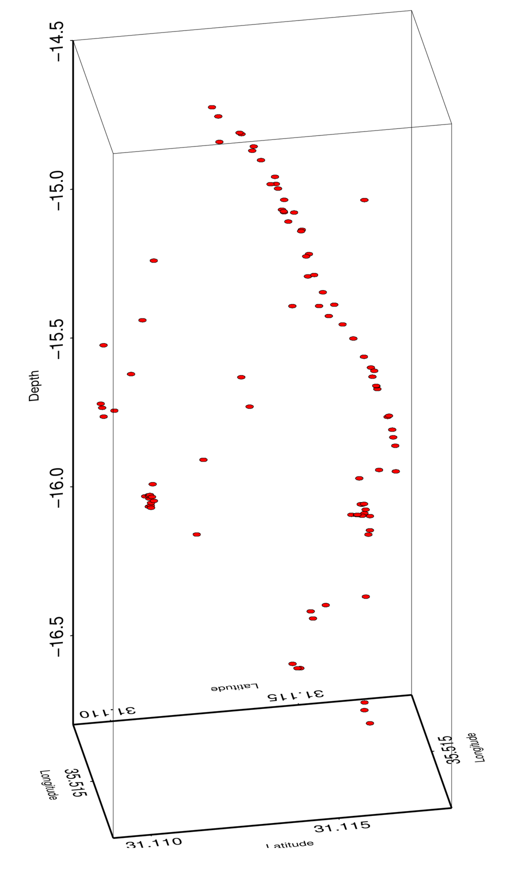

Fig. 8 The events of the cluster in a 3D plot. No vertical exaggeration.

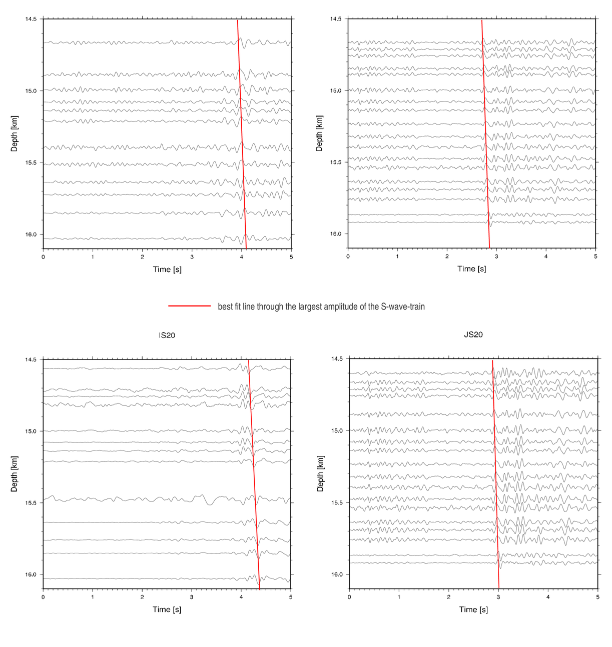

Fig. 9 For some high quality events in different depths, the waveforms are aligned to the P onsets. The waveforms are then displayed at their depth determined by HypoDD. The red line is indicating the best fit line through the largest amplitude of the S-wave-train. With increasing depth the distance between P and S onset is increasing. Thus, the depth distribution of the relocated events seems not to be an artefact of the relocation procedure.

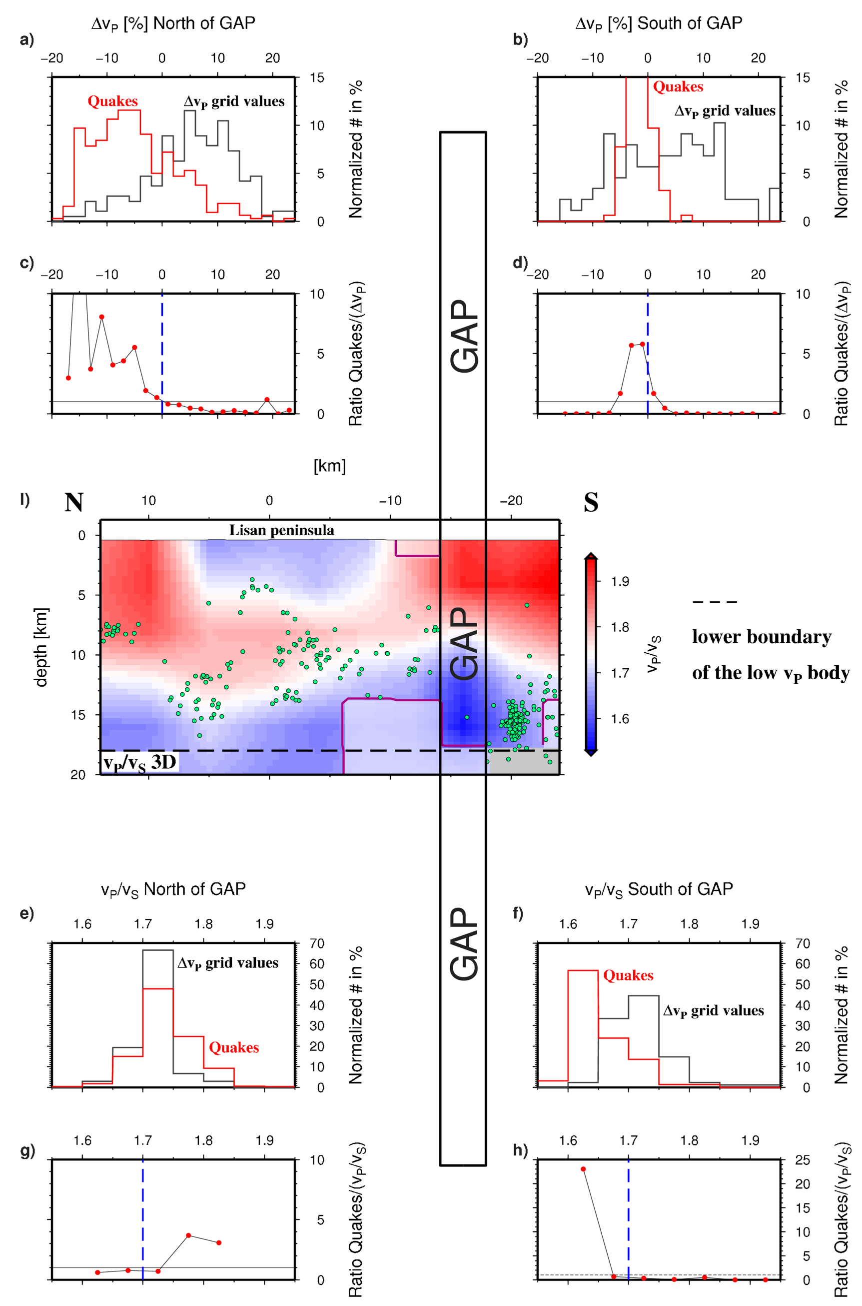

Fig. 10
For a quantitative verification we use the approach of Hauksson (2011), assuming that geophysical parameters are not uniformly distributed. Thus, it needs to be verified whether the preferred earthquake occurrence in a certain range of a geophysical parameter is not just a result of the general frequency of this parameter range. Therefore, the normalized number of the occurrence of a unit of a certain parameter (here Δv_P and v_P/v_S) within the whole inversion grid is plotted as a histogram together with the histogram of the normalized numbers of earthquakes for the same unit of the parameter value (a, b, e, f). The two normalized histograms are divided (divided red by black) to obtain the ratio of earthquakes per unit of the chosen parameter ((Hauksson, 2011), c, d, g, h). North-South depth section (for exact location see Figure 1) through the 3-D model of the v_P/v_S ratios in the eastern edge of the DSB from Braeuer et al. (2012) with earthquakes around the section as green dots (I).
Following Braeuer et al. (2012) the basin-fill sediments are characterized by low P-velocities and high v_P/v_S ratios. Thus the events North of the GAP are occurring mainly within the basin-fill sediments (c, g). However, the activity South of the GAP occurs below the basin-fill sediments - where the P-velocity is still low (d) but the v_P/v_S ratios are low (h)

Fig. 11
a) Map of the study area, rotated 8° ccw to align approximately with the direction of the main border faults; b) Projected hypocentres on a vertical cross-section along the main axis of the DSB; c) Projected hypocentres on a vertical cross-section along the transverse axis of the DSB; d) Histogram of events per depth kilometer. The events, marked as dots in different colours, scaled by its magnitude. For each different seismic region one or two characteristic focal mechanism are indicated. The three main regions of different seismic activity A, B and C marked. A is representing the seismic activity South of the Bokek fault which is solely related to the eastern boundary fault (EBF). These events occur mainly in the depth range from 12 to 18 km and its focal plane solutions are showing strike-slip mechanisms (see Figure 5). The spatial and temporal cluster in February 2007 (Figures 6-9) occurred also South of the seismically inactive region (GAP). B is representing the upper crustal activity North of the GAP, occurring at both boundaries in the same depth range between 4 and 17 km (see Figure 3) and with similar focal mechanisms (normal and strike-slip, see Figure 5). Furthermore, the activity in the lower crust in the depth range of 25 – 29 km is marked with C.

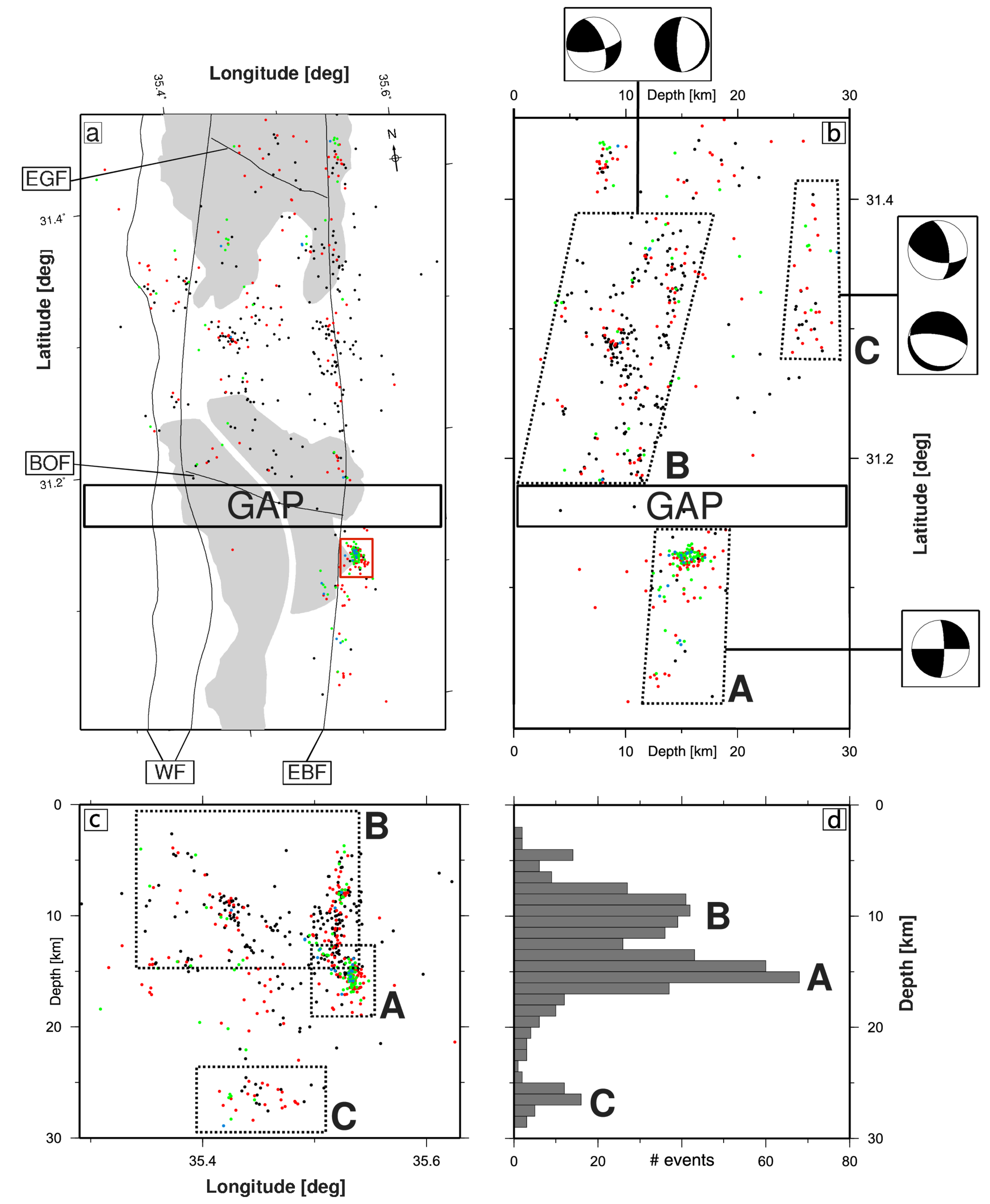

Discussion

For the determination of accurate hypocenters and focal mechanisms in the study area, event locations revealed through a tomographic inversion (2-D or 3-D) are essential (Figure 2). Crustal earthquakes occur from 2 to 29 km depth, while large part of the seismicity is concentrated in the upper crust down to 20 km depth (Figure 11). The determined b-value of 0.7 indicates a relatively high risk of large earthquakes compared to the moderate microseismic activity (Figure 4).
The distribution of the seismicity is confirming the velocity models presented in Braeuer et al. (2012), indicating an asymmetric basin due to the transtensional regime of the region (Garfunkel, 1981; Smit et al., 2010), with a vertical strike-slip fault forming the eastern boundary, and an inclined western boundary, made up of strike-slip and normal faults (Figure 11c).
The seismic behavior exhibit significant differences between the area North and South of the Bokek fault (GAP in Figures 10, 11). South of the Bokek fault the western boundary is inactive while the entire seismicity occurs at the eastern boundary (Figure 3) and below the basin-fill sediments (Figure 10). The largest events occurred here, their focal mechanisms represent the northwards transform motion of the Arabian plate along the Dead Sea Transform (Figure 5). The vertical extension of the the spatial and temporal cluster from February 2007 (Figure 6-9) is probably related to the locking of the region around the Bokek fault (GAP in Figures 10,11). North of the Bokek fault similar seismic activity occurs at both boundaries (Figure 3) most notably within the basin-fill sediments (Figure 10), displaying mainly small events with strike-slip mechanism and normal faulting in EW direction (Figure 5). Therefore, we suggest that the Bokek fault forms the actual border between the transform activity and the pull-apart basin.

References

Braeuer, B.; Asch, G.; Hofstetter, R.; Haberland, C.; Jaser, D.; El-Kelani, R.; Weber, M. (2012): High-resolution local earthquake tomography of the southern Dead Sea area.. Geophysical Journal International, 191, 3, 881-897.

Garfunkel, Z. 1981. Internal structure of the Dead Sea leaky transform (rift) in relation to plate kinematics. Tectonophysics, 80, 81-108.

Y. Hamiel and R. Amit and Z. B. Begin and S. Marco and O. Katz and A. Salamon and E. Zilbermann and N. Porat, The Seismicity along the Dead Sea Fault during the Last 60 000 Years, Bull. Seismol. Soc. Am. (2009), pp. 2020-2026

References

E. Hauksson, Crustal geophysics and seismicity in southern California, J. Geophys. Res. (2011), pp. 82—98

A. Shapira and L. Feldman, Microseismicity of three locations along the Jordan Rift, Tectonophysics (1987), pp. 89—94

J. Smit and J.-P. Brun and S. Cloetingh and Z. Ben-Avraham, The rift-like structure and asymmetry of the Dead Sea Fault, Earth Plan. Sci. Lett. (2010), pp. 74—82

Waldhauser, F. (2001). HypoDD: a program to compute double-difference hypocenter locations, U.S. Geol. Surv. Open-File Rept. 01-113, Menlo Park, California.

Acknowledgments

We thank the National Ministry of Infrastructure of Israel, the Natural Resources Authority of Jordan and the An-Najah University in Nablus, the Palestine Territories for their support throughout this project. We thank the military, security, and customs agencies of Israel and Jordan for their help and our contractors the Geophysical Institute of Israel and the Chemical and Mining Industries (Jordan) for their excellent work under difficult logistic conditions. The seismic instruments were provided by the Geophysical Instrument Pool of the GeoForschungsZentrum Potsdam and IRIS/PASSCAL, USA. The DESIRE project was funded by the Deutsche Forschungsgemeinschaft.